Journal of Nanostructure in Chemistry
a SpringerOpen Journal

ORIGINAL Open Access

# Simple preparation of ferromagnetic $Co_3O_4$ nanoparticles by thermal dissociation of the $[Co^{II}(NH_3)_6](NO_3)_2$ complex at low temperature

Saeid Farhadi*, Kolsoum Pourzare and Shokooh Sadeghinejad

**Abstract**

$Co_3O_4$ nanoparticles were prepared using $[Co(NH_3)_6](NO_3)_2$ as a starting material via a solid-state thermal decomposition route at low temperature (150°C). The product was characterized by thermal analysis (thermogravimetric/derivative thermogravimetric/differential thermal analysis), X-ray diffraction, Fourier transform infrared spectroscopy, Raman spectroscopy, Brunauer-Emmett-Teller specific surface area measurement, UV-visible spectroscopy, transmission electron microscopy (TEM), energy-dispersive X-ray spectroscopy, and magnetic measurements. The results confirmed that the nanoparticles are highly pure $Co_3O_4$ with weak ferromagnetic properties. TEM images showed that the $Co_3O_4$ nanoparticles have an average diameter size of around 13 nm. The optical spectrum indicated two direct bandgaps at 2.3 and 3.2 eV which are blueshifted relative to reported values for the bulk sample. By this fast and simple method, $Co_3O_4$ nanoparticles can be produced without expensive and toxic solvents or complicated equipment.

**Keywords:** Thermal dissociation, Co(II) complex, Nanoparticles, Cobalt oxide, Magnetic properties, Optical properties

## Background

Transition metal oxide nanoparticles represent a broad class of materials that have been investigated extensively due to their interesting catalytic, electronic, and magnetic properties relative to those of the bulk counterparts, and the wide scope of their potential applications [1-4]. Among metal oxides, special attention has been focused on the synthesis and properties of spinel-type $Co_3O_4$ which is important as a heterogeneous catalyst, solid-state sensor, anode material in Li-ion rechargeable batteries, pigment, electrochromic sensor, and magnetic material and in solar energy storage [5-12]. For these diverse applications, it is of great importance to prepare $Co_3O_4$ with well-controlled dimensionality, sizes, and crystal structure. Up to now, several methods have been reported in order to synthesize $Co_3O_4$ nanoparticles, including sol–gel method [13], hydrothermal method [14,15], combustion method [16], microemulsion method [17], chemical spray pyrolysis [18], chemical vapor deposition [19,20], thermal decomposition of cobalt precursors [21-26], sonochemical route [27,28], co-precipitation [29], microwave irradiation [30], and mechanochemical processing [31]. However, most of these methods have one or more drawbacks, such as prolonged reaction times, the use of toxic and expensive solvents/reagents, complicated synthetic steps, the use of expensive equipment, and high synthetic temperatures. Therefore, the development of simple, inexpensive, and nontoxic methods for the preparation $Co_3O_4$ nanoparticles at relatively low temperature is still demanded.

Among the numerous methods developed for preparing metal oxide nanomaterials, the molecular precursor route has been regarded as one of the most convenient and practical techniques because it not only enables to avoid special instruments, complicated processes, and severe preparation conditions but also provides good control over purity, homogeneity, composition, phase, and microstructure of the resultant products [32-39]. By choosing a proper molecular precursor, coupled with a rational calcining procedure or other decomposition processes [40-43], nanocrystalline products could be obtained usually under the conditions significantly milder than those employed in the conventional solid-state synthesis.

Herein, we report on the preparation of $Co_3O_4$ nanoparticles by direct solid-state thermal dissociation of the

* Correspondence: sfarhadi48@yahoo.com
Department of Chemistry, Lorestan University, Khoramabad 68135-465, Iran

Springer

© 2013 Farhadi et al.; licensee Springer. This is an Open Access article distributed under the terms of the Creative Commons Attribution License (http://creativecommons.org/licenses/by/2.0), which permits unrestricted use, distribution, and reproduction in any medium, provided the original work is properly cited.

labile $[Co(NH_3)_6](NO_3)_2$ complex as a new precursor, as well as the characterization of the obtained product by X-ray diffraction (XRD), Fourier transform infrared spectroscopy (FT-IR), Raman spectroscopy, UV-visible (UV–vis) spectroscopy, Brunauer-Emmett-Teller (BET) specific surface area measurement, energy-dispersive X-ray spectroscopy (EDX), transmission electron microscopy (TEM), thermal analysis (thermogravimetric(TG)/derivative thermogravimetric (DTG)/differential thermal analysis (DTA)), and magnetic measurements.

## Results and discussion

First, the thermal behavior of the $[Co(NH_3)_6](NO_3)_2$ precursor was studied by thermal analysis. Figure 1 shows TG, DTG, and DTA curves recorded for $[Co(NH_3)_6](NO_3)_2$ at a constant heating rate of 10°C $min^{-1}$in the temperature range of 25°C to 600°C. The TG and DTG curves show that the decomposition of the complex proceeds in two main stages. The first stage that occurred at about 100°C shows 12.20% weight loss which is consistent with the theoretical value of 11.95% caused by the loss of two molecules of $NH_3$ per one molecule of the complex. In the second stage, an extensive weight loss (60%) is observed at about 150°C, which related to the decomposition of the residue $[Co(NH_3)_4](NO_3)_2$ complex. Above 150°C, the weight remained constant, confirming the complete decomposition of the complex. The weight loss of all steps is about 72% which is consistent with the theoretical value (71.85%) calculated for the formation of $Co_3O_4$ from the complex. The DTA curve in the inset of Figure 1 shows two characteristic peaks. The small endothermic peak at about 100°C can be explained by freeing two $NH_3$ molecules in consistent with TG and DTG data. The residue gives a sharp exothermic peak at about 150°C. This exothermic peak related to the explosive decomposition of the complex via an intramolecular redox process occurring between the reductants ($NH_3$ ligands) and the oxidants ($NO_3^-$). The explosive decomposition of the complex resulted in the solid $Co_3O_4$ and gaseous products, i.e., $NH_3$, $N_2$, NO, $N_2O$, and $H_2O$. Although not all of the reaction products were determined in the analyses, the decomposition of the complex and formation of the $Co_3O_4$ nanoparticles can be expressed as follows:

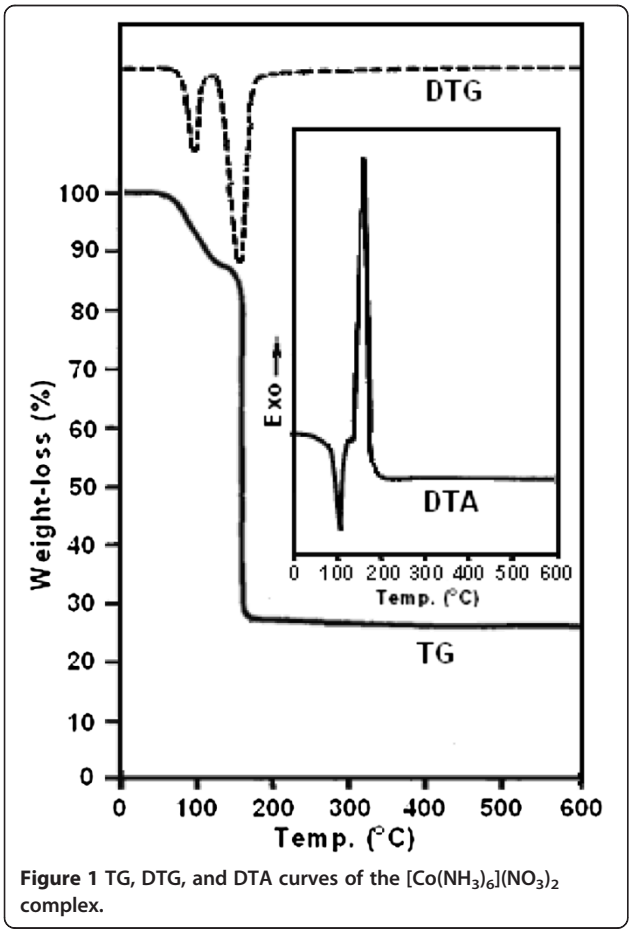


**Figure 1** TG, DTG, and DTA curves of the $[Co(NH_3)_6](NO_3)_2$ complex.

$$9[Co(NH_3)_6](NO_3)_2(s) \rightarrow 3Co_3O_4(s) + 30NH_3(g) + 4NO(g) + 2N_2O(g) + 17N_2(g) + 36H_2O(g)$$

Figure 2 shows FT-IR spectra of the $[Co(NH_3)_6](NO_3)_2$ complex and its decomposition products at different temperatures. In Figure 2(spectrum a), the characteristic stretching bands of $NH_3$ and $NO_3$ groups are observed at about 3,500 to 3,000, 1,600, 1,350, and 800 $cm^{-1}$[44]. As shown in Figure 2(spectrum b), all the bands associated with the complex clearly disappeared when the complex was decomposed at 150°C. At this temperature, only two characteristic strong bands of the spinel-type $Co_3O_4$ structure at about 663.47 and 570.89 $cm^{-1}$ are observed [45], confirming that the complex was decomposed completely at 150°C to the $Co_3O_4$ phase as indicated by the TG/DTA results. In Figure 2(spectrum c), the FT-IR spectrum of the sample decomposed at 175°C shows the strong bands related to $Co_3O_4$ without obvious change.

Figure 3 presents the XRD patterns of the decomposition products of the $[Co(NH_3)_6](NO_3)_2$ complex at 150°C and 175°C. Well-defined diffraction peaks at about 19.52°, 31.50°, 37.05°, 38.77°, 44.96°, 55.80°, 59.53°, 65.30°, 74.55°, 77.50°, and 78.60° are observed, corresponding to the (111), (220), (311), (222), (400), (422), (511), (440), (620), (533), and (622) planes of $Co_3O_4$ crystals, respectively (JCPDS card no. 76–1802). This result confirms that the complex was decomposed completely into the $Co_3O_4$ phase at 150°C, in good agreement with the thermal analysis and FT-IR results. No impurity peaks were found in the XRD patterns, confirming that the product is well-crystallized $Co_3O_4$ with high purity. As can be seen, the diffraction peaks are broadened because of the small size effect of the nanoparticles. The average crystallite size ($d$) was calculated to be approximately 13 nm by the Scherrer

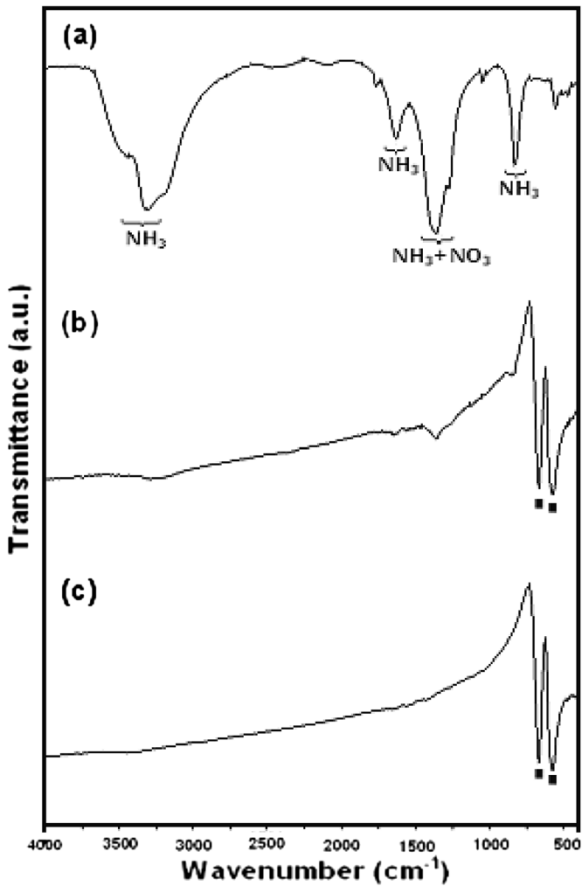


**Figure 2 FT-IR spectra of (a) the $[Co(NH_3)_6](NO_3)_2$ complex and its decomposed products at (b) 150°C and (c) 175°C.** The black-filled square indicates the $Co_3O_4$ phase.

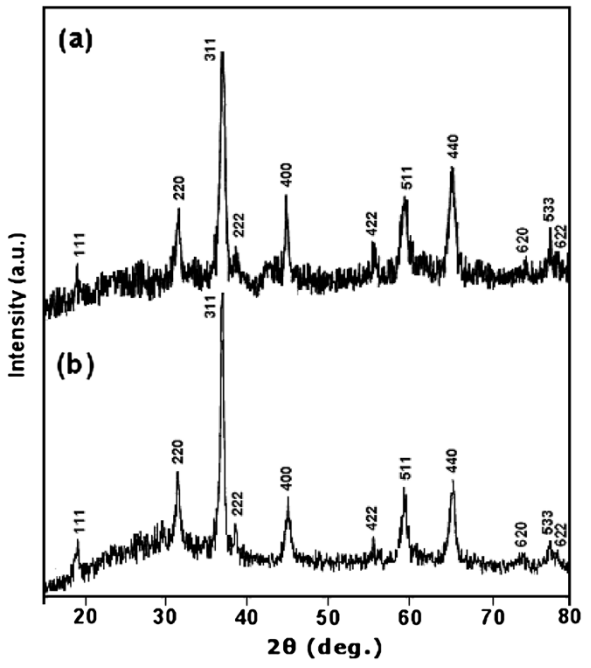


**Figure 3 XRD patterns of the $[Co(NH_3)_6](NO_3)_2$ complex decomposed at (a) 150°C and (b) 175°C.**

relation [46]: $d = 0.9\lambda/(B\cos\theta)$, where $\lambda$ is the wavelength of Cu Kα radiation, $B$ is the corrected full width at half maximum of the diffraction peak, and $\theta$ is the Bragg angle. As shown in Figure 3 (pattern b), no new phase was observed when the decomposition temperature increased to 175°C, but the width of the $Co_3O_4$ peaks decreased because of crystallite growth.

Figure 4 displays the Raman spectrum of the $Co_3O_4$ nanoparticles. As shown in Figure 4, the Raman spectrum of the $Co_3O_4$ nanoparticles in the range of 300 to 800 nm shows four obvious peaks located at around 468, 510, 605, and 670 $cm^{-1}$, corresponding to the four Raman-active modes ($A_{1g}$, $E_g$, and $2F_{2g}$) of $Co_3O_4$. The Raman shifts are consistent with those of pure crystalline $Co_3O_4$[47,48], indicating that the $Co_3O_4$ nanoparticles have a similar crystal structure to bulk $Co_3O_4$. However, compared with those for bulk $Co_3O_4$, the peak positions of the four active modes shift to low wavenumbers by about 10 to 20 $cm^{-1}$ [49]. This phenomenon is attributed to the optical phonon confinement effect in nanostructures, which can cause uncertainty in the phonon wave vectors and thus a downshift in the Raman peaks [50]. This result further confirms the formation of the $Co_3O_4$ nanoparticles.

Figure 5 shows TEM images of the $Co_3O_4$ powder prepared by thermal decomposition of the $[Co(NH_3)_6](NO_3)_2$ complex at 150°C. The TEM sample was prepared by dispersing the powder in ethanol by ultrasonic vibration. It can be seen that the product was formed from extremely fine spherical particles which were loosely aggregated. The uniform $Co_3O_4$ particles have sphere-like shapes with weak agglomeration. As can be seen in the inset of Figure 5, the particle sizes possess a narrow distribution in a range of 6 to 20 nm, and the mean particle diameter is about 13 nm. In fact, the mean particle size determined by

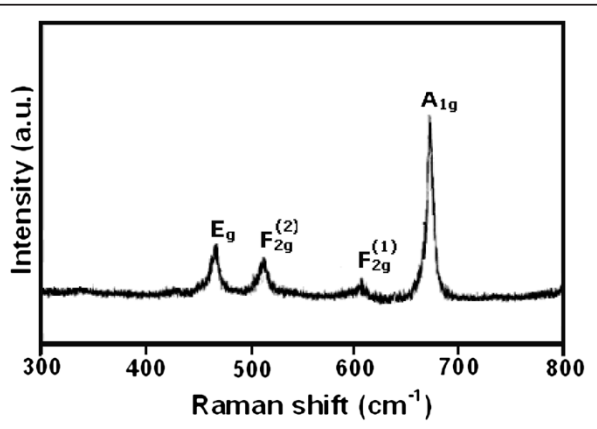


**Figure 4 Raman spectrum of the $Co_3O_4$ nanoparticles.**

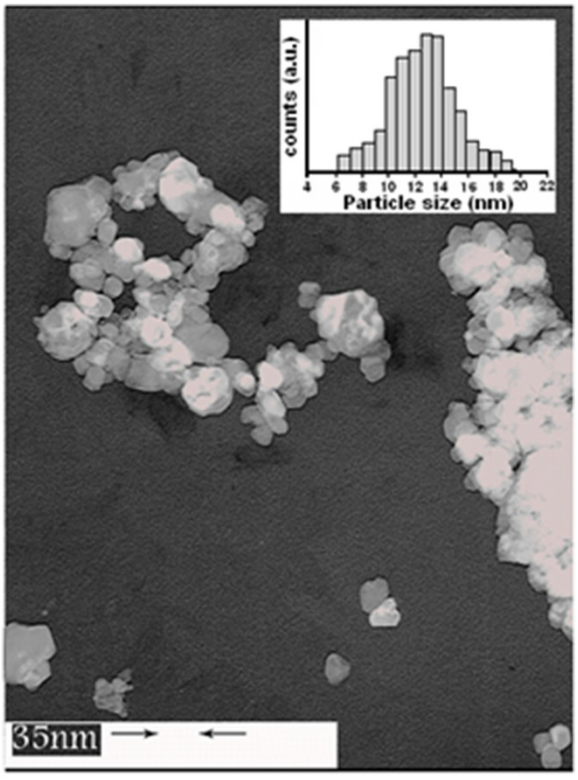


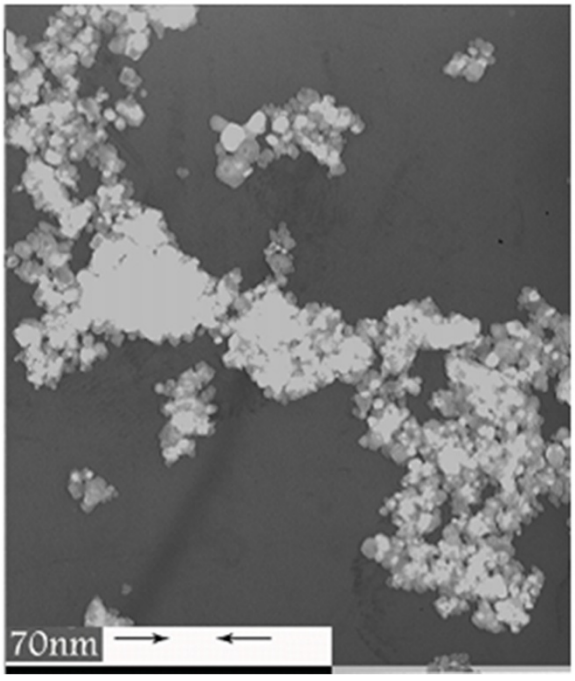


**Figure 5 TEM images of the $Co_3O_4$ nanoparticles in two different magnifications.** The inset shows the particle size distribution of $Co_3O_4$ nanoparticles.

TEM is very close to the average particle size calculated by the Debye-Scherer formula from the XRD pattern.

The EDX spectrum of the product in Figure 6 reveals the presence of only cobalt and oxygen peaks, with no other relevant elements present; the large Si peak can be attributed to the Si wafer upon which the nanoparticles were deposited prior to analysis. The atomic percentages of Co and O were found to be 43.15% and 56.95%, respectively. The atomic ratio of Co and O is 3:3.96, which approaches the theoretical value for $Co_3O_4$. This observation further confirms that the final product is only highly pure $Co_3O_4$ nanoparticles.

The surface area of the $Co_3O_4$ nanoparticles obtained from the decomposition of the complex was measured by the BET method. The specific surface area of the sample was 77.50 $m^2/g$. Assuming that the nanoparticles are almost spherical, as confirmed by TEM, the surface area can be used to estimate the particle size according to $D_{BET} = 6{,}000/(\rho \times S_{BET})$, where $D_{BET}$ is the diameter of a spherical particle (nm), $\rho$ is the theoretical density of $Co_3O_4$ (6.05 $g/cm^3$), and $S_{BET}$ is the specific surface area of $Co_3O_4$ powder ($m^2/g$). The particle size calculated from the surface area data is about 12.80 nm, which is in good agreement with the XRD and TEM results.

The optical absorption properties of the as-prepared $Co_3O_4$ nanoparticles were investigated at room temperature by UV–vis spectroscopy (Figure 7). There are two obvious absorption peaks at 281 and 531 nm. $Co_3O_4$ is a p-type semiconductor, and its optical bandgap can be obtained from the following equation [16]: $(Ahv)^n = B(hv - E_g)$, where $hv$ is the photon energy (eV), $A$ is the absorption coefficient, $B$ is a constant relative to the material, $E_g$ is the bandgap, and $n$ is either 1/2 for an indirect transition or 2 for a direct transition. The $(Ahv)^2$ versus $hv$ curve for the product is shown in the inset of Figure 7. The value of $hv$ extrapolated to $(Ahv)^2 = 0$ gives the absorption bandgap energy. Two regions with a linear relationship are observed in the ranges of 3.8 to 6.1 and 1.9 to 2.5, respectively, giving two $E_g$ values of 3.2 and 2.3 eV.

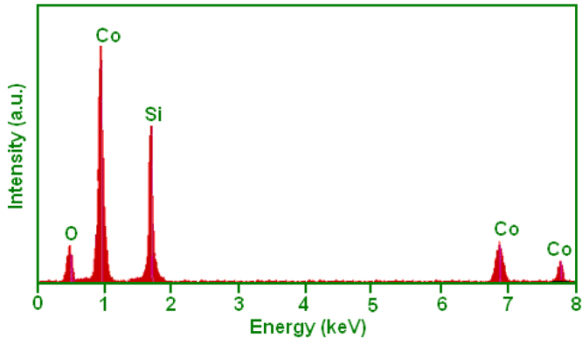


**Figure 6 EDX analysis of the $Co_3O_4$ nanoparticles.**

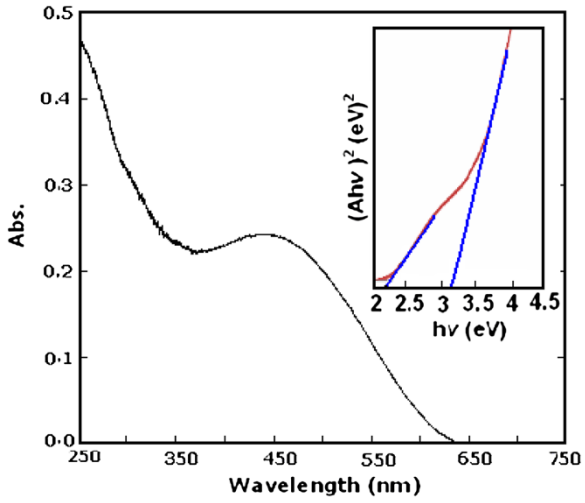


**Figure 7 UV–vis spectrum and $(Ahv)^2$-$hv$ curve (inset) of the $Co_3O_4$ nanoparticles prepared at 150°C.**

The bandgap of 2.3 eV can be associated with the $O^{II-} \rightarrow Co^{II}$ charge transfer process (valence to conduction band excitation), while the 3.2 eV bandgap relates to the $O^{II-} \rightarrow Co^{III}$ charge transfer (with the $Co^{III}$ level located below the conduction band) [51]. As has been investigated in the literatures [27,52], the $E_g$ values of $Co_3O_4$ nanoparticles are greater than those of bulk $Co_3O_4$ ($E_g$=1.77 and 3.17 eV, respectively). The increase in the bandgap of the $Co_3O_4$ nanoparticles may ascribe to the quantum confinement effects of nanomaterials.

Figure 8 shows the magnetic properties of the $Co_3O_4$ nanoparticles. The fine shape of the hysteresis loops is a characteristic of a weak ferromagnetic behavior, although bulk $Co_3O_4$ is antiferromagnetic [53]. From the inset, the coercive field ($H_c$) and the remanent magnetization ($M_r$) are estimated to be 0.015 kOe and 0.002 emu/g, respectively. The low coercive fields and remanent magnetizations confirm that the $Co_3O_4$ nanoparticles have weak ferromagnetic properties. The maximum applied field, 8 kOe, does not saturate the magnetizations which should be attributed to weak ferromagnetic ordering of the spins in the nanoparticles. $Co_3O_4$ nanoparticles consist of small magnetic domains, each characterized by its own randomly oriented magnetic moment. The total magnetic moment of the nanoparticles is the sum of these magnetic domains coupled by dipolar interactions. The ferromagnetic behavior of the $Co_3O_4$ nanoparticles can be explained as follows: bulk $Co_3O_4$ has a normal spinel structure with antiferromagnetic exchange between ions occupying tetrahedral and octahedral sites [53]. It has zero net magnetization due to the complete compensation of sublattice magnetizations. Hence, the change from an antiferromagnetic state for bulk $Co_3O_4$ to a weakly ferromagnetic state for $Co_3O_4$ nanoparticles can be ascribed to uncompensated surface spins and/or finite size effects [54,55].

## Conclusions

In this work, we presented a simple and low-temperature method of synthesizing spinel-type $Co_3O_4$ nanoparticles with an average particle size of 13.5 nm through thermolysis of the $[Co(NH_3)_6](NO_3)_2$ at low temperature (150°C). $Co_3O_4$ nanoparticles are formed from this complex via an explosive redox reaction between $NH_3$ ligands as the

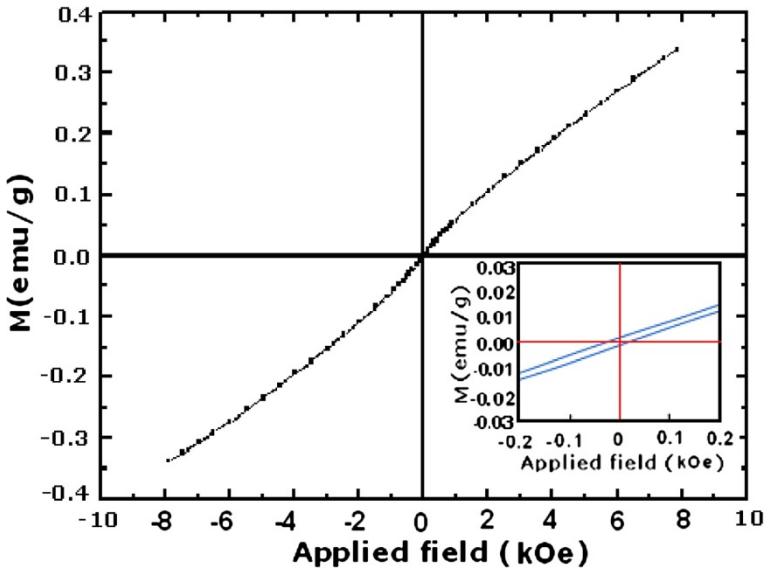


**Figure 8 Magnetization vs. field ($M$-$H$) of $Co_3O_4$ nanoparticles prepared from $[Co(NH_3)_6](NO_3)_2$ precursor at 150°C.** The inset shows its expansion of magnetization vs. field near the lower applied field.

reducing agent and the $NO_3^-$ ions acting as the oxidizing agent. This method yields sphere-like $Co_3O_4$ nanoparticles with weak agglomeration, a narrow size distribution, and weak ferromagnetic behavior. The estimated optical absorption bandgaps of the $Co_3O_4$ nanoparticles were about 2.3 and 3.2 eV, which are relatively blueshifted, compared with the values for the bulk sample. This approach provides a one-step, general, and inexpensive route for the preparation of $Co_3O_4$ nanoparticles with high purity for industrial and high-technology applications.

## Methods

### Preparation of $Co_3O_4$ nanoparticles

Initially, the $[Co(NH_3)_6](NO_3)_2$ complex was synthesized via a simple reaction of an aqueous solution of $[Co(H_2O)_6](NO_3)_2$ with concentrated ammonia solution according to the reported method [56]. By adding acetone to the reaction mixture, the complex was precipitated as an orange precipitate. The composition of the complex was confirmed by thermal analysis, FT-IR, and elemental analysis: anal. calc. for $[Co(NH_3)_6](NO_3)_2$: Co, 20.68; H, 6.32; N, 39.30; found: Co, 21.10; H, 6.25; N, 39.89. To prepare $Co_3O_4$ nanoparticles, the $[Co(NH_3)_6](NO_3)_2$ complex was decomposed at selected temperatures for 1 h in an electric furnace under ambient air. The temperatures were selected according to the thermoanalytical data. The decomposition product was collected for characterization.

### Characterization techniques

The XRD patterns were recorded by a Rigaku D-max C III X-ray diffractometer (Rigaku Corporation, Shibuya-ku, Japan) using Ni-filtered Cu Kα radiation ($\lambda$ = 1.5418 Å) in order to determine the phases present in the decomposed samples. Infrared spectra were recorded on a Schimadzu system 160 FT-IR spectrophotometer (Shimadzu Corporation, Kyoto, Japan) using KBr pellets. The Raman spectra were measured on a Spex 1403 Raman spectrometer. Thermal analysis was conducted with a Netzsch STA 409 PC/PG thermal analyzer at a heating rate of 5°C $min^{-1}$ in air. The optical absorption spectrum was recorded on a Shimadzu 1650PC UV–vis spectrophotometer in a wavelength range of 200 to 700 nm at room temperature. The sample for UV–vis studies was well dispersed in distilled water to form a homogeneous suspension by sonication for 25 min. The particle size was determined using a transmission electron microscope (Philips CM10, Philips, Amsterdam, The Netherlands) equipped with an energy dispersive X-ray analyzer. For the TEM measurements, the powders were ultrasonicated in ethanol, and a drop of the suspension was dried on a carbon-coated microgrid. The specific surface area of the product was measured by the BET method using $N_2$ adsorption-desorption isotherm carried out at −196°C on a surface area analyzer (Micromeritics ASAP 2010, Micromeritics, Norcross, GA, USA). Before each measurement, the sample was degassed at 150°C for 2 h. A vibrating sample magnetometer (Meghnatis Daghigh Kavir Co., Kashan, Iran) was used to measure the magnetic properties of $Co_3O_4$ nanoparticles.

#### Competing interests

The authors declare that they have no competing interests.

#### Authors' contributions

SF participated in the idea of the study, the design of the study, interpretation of the results, and writing the manuscript for publication. KP carried out the synthesis and the physicochemical characterization of the $Co_3O_4$ nanoparticles and early drafted the manuscript. SS participated in the discussions and interpretation of all characterization results. All authors read and approved the final manuscript.

#### Authors' information

SF is a professor at the Department of Chemistry, Lorestan University, Iran. He received his BSc degree in Chemistry from Shahid Chamran University in 1991, his MSc degree in Inorganic Chemistry from Tehran University in 1994, and his Ph.D. in Inorganic Chemistry from Isfahan University, Iran, in 2000. His recent research has concentrated on synthesis and characterization of metal and metal oxides nanostructures, and their catalytic applications. KP obtained her BSc and MSc degrees in Chemistry from the Faculty of Science, Lorestan University, Iran, in 2008 and 2012, respectively. During her MSc course, she has been involved in synthesizing cobalt oxide nanostructures through thermal decomposition of some ammine complexes. Her research interest is in the area of nanomaterial preparation. SS obtained her BSc degree in Applied Chemistry in 2009 from the Faculty of Science, Arak University, Iran. She earned her MSc degree in Inorganic Chemistry in 2012 with the thesis entitled 'Preparation and characterization of silver nanoparticles via chemical reduction with hydrogen peroxide ($H_2O_2$),' from the Faculty of Science, Lorestan University, Iran. Her research area interests include metals and metal oxide nanomaterials.

#### Acknowledgements

This work was supported by the Lorestan University Research Council and also supported by Iran Nanotechnology Initiative Council (INIC).

Received: 25 August 2012 Accepted: 4 April 2013
Published: 20 April 2013

#### References

1. He, JH, Wu, TH, Hsin, CL, Li, KM, Chen, LJ, Chueh, YL: Beak-like $SnO_2$ nanorods with strong photoluminescent and field-emission properties. Small **2**, 116–120 (2006)
2. Xu, LP, Sithambaram, S, Zhang, YS, Chen, CH, Jin, L, Joesten, R, Suib, SL: Novel urchin-like CuO synthesized by a facile reflux method with efficient olefin epoxidation catalytic performance. Chem. Mater. **21**, 1253–1259 (2009)
3. Hu, CC, Wu, YT, Chang, KH: Low-temperature hydrothermal synthesis of $Mn_3O_4$ and MnOOH single crystals: determinant influence of oxidants. Chem. Mater. **20**, 2890–2894 (2008)
4. Zhou, J, Ding, Y, Deng, SZ, Gong, L, Xu, NS, Wang, ZL: Three-dimensional tungsten oxide nanowire networks. Adv. Mater. **17**, 2107–2110 (2005)
5. Lou, XW, Deng, D, Lee, JY, Feng, J, Archer, LA: Self-supported formation of needlelike $Co_3O_4$ nanotubes and their application as lithium-ion battery electrodes. Adv. Mater. **20**, 258–262 (2008)
6. Casas-Cabanas, M, Binotto, G, Larcher, D, Lecup, A, Giordani, V, Tarascon, JM: Defect chemistry and catalytic activity of nanosized $Co_3O_4$. Chem. Mater. **21**, 1939–1947 (2009)
7. Li, W-Y, Xu, L-N, Chen, J: $Co_3O_4$ nanomaterials in lithium-ion batteries and gas sensors. Adv. Funct. Mater. **15**, 851–857 (2005)
8. Chou, S-L, Wang, J-Z, Liu, H-K, Dou, S-X: Electrochemical deposition of porous $Co_3O_4$ nanostructured thin film for lithium-ion battery. J. Power. Sources **182**, 359–364 (2008)
9. Askarinejad, A, Bagherzadeh, M, Morsali, A: Catalytic performance of $Mn_3O_4$ and $Co_3O_4$ nanocrystals prepared by sonochemical method in epoxidation of styrene and cyclooctene. Appl. Surface Sci. **256**, 6678–6682 (2010)

10. Li, YG, Tan, B, Wu, YY: Mesoporous $Co_3O_4$ nanowire arrays for lithium ion batteries with high capacity and rate capacity. Nano Lett. **8**, 265–270 (2008)
11. Mate, VR, Shirai, M, Rode, CV: Heterogeneous $Co_3O_4$ catalyst for selective oxidation of aqueous veratryl alcohol using molecular oxygen. Catal. Commun. **33**, 66–69 (2013)
12. Makhlouf, SA: Magnetic properties of $Co_3O_4$ nanoparticles. J. Magn. Magn. Mater. **246**, 184–190 (2002)
13. Baydi, ME, Poillerat, G, Rehspringer, JL, Gautier, JL, Koenig, JF, Chartier, P: A sol–gel route for the preparation of $Co_3O_4$ catalyst for oxygen electrocatalysis in alkaline medium. J. Solid State Chem. **109**, 281–288 (1994)
14. Chen, Y, Zhang, Y, Fu, S: Synthesis and characterization of $Co_3O_4$ hollow spheres. Mater. Lett. **61**, 701–705 (2007)
15. Li, L, Chu, Y, Liu, Y, Song, JL, Wang, D, Du, XW: A facile hydrothermal route to synthesize novel $Co_3O_4$ nanoplates. Mater. Lett. **62**, 1507–1510 (2008)
16. Gu, F, Li, C, Hu, Y, Zhang, L: Synthesis and optical characterization of $Co_3O_4$ nanocrystals. J. Cryst. Growth **304**, 369–373 (2007)
17. Wang, RM, Liu, CM, Zhang, HZ, Chen, CP, Guo, L, Xu, HB, Yang, SH: Porous nanotubes of $Co_3O_4$: synthesis, characterization and magnetic properties. Appl. Phys. Lett. **85**, 2080–2082 (2004)
18. Kim, DY, Ju, SH, Koo, HY, Hong, SK, Kangf, YC: Synthesis of nanosized $Co_3O_4$ particles by spray pyrolysis. J. Alloys Compd. **417**, 254–258 (2006)
19. Mane, AU, Shalini, K, Wohlfart, A, Devi, A, Shivashankar, SA: Strongly oriented thin films of $Co_3O_4$ deposited on single-crystal MgO(100) by low-pressure, low-temperature MOCVD. J. Cryst. Growth **240**, 157–163 (2002)
20. Xuan, Y, Liu, R, Jia, YQ: Synthesis of a new series of compounds $RE_2Co_{2/3}Nb_{4/3}O_7$ and stability field diagram of $RE_2B_{2/3}{}'B_{4/3}{}''O_7$ pyrochlore compounds. Mater. Chem. Phys. **53**, 256–261 (1998)
21. Rumplecker, A, Kleitz, F, Salabas, EL, Schüth, F: Hard templating pathways for the synthesis of nanostructured porous $Co_3O_4$. Chem. Mater. **19**, 485–496 (2007)
22. Wang, WW, Zhu, YJ: Microwave-assisted synthesis of cobalt oxalate nanorods and their thermal conversion to $Co_3O_4$ rods. Mater. Res. Bull. **40**, 1929–1935 (2005)
23. Yang, LX, Zhu, YJ, Li, L, Zhang, L, Tong, H, Wang, WW: A facile hydrothermal route to flower-like cobalt hydroxide and oxide. Eur. J. Inorg. Chem. **23**, 4787–4792 (2006)
24. Mohandes, F, Davar, F, Salavati-Niasari, M: Preparation of $Co_3O_4$ nanoparticles by nonhydrolytic thermolysis of $[Co(Pht)(H_2O)]_n$ polymers. J. Magn. Magn. Mater. **322**, 872–877 (2010)
25. Jiang, J, Li, L: Synthesis of sphere-like $Co_3O_4$ nanocrystals via a simple polyol route. Mater. Lett. **61**, 4894–4896 (2007)
26. Ren, L, Wang, P, Han, Y, Hu, C, Wei, B: Synthesis of $CoC_2O_4{\cdot}2H_2O$ nanorods and their thermal decomposition to $Co_3O_4$ nanoparticles. Mater. Phys. Lett. **476**, 78–83 (2009)
27. Kumar, RV, Diamant, Y, Gedanken, A: Synthesis and characterization of nanometer-size transition metal oxides from metal acetates. Chem. Mater. **12**, 2301–2305 (2000)
28. Oh, SW, Bang, HJ, Bae, YC, Sun, Y-K: Effect of calcination temperature on morphology, crystallinity and electrochemical properties of nano-crystalline metal oxides ($Co_3O_4$, CuO, and NiO) prepared via ultrasonic spray pyrolysis. J. Power. Sources **173**, 502–509 (2007)
29. Lai, T, Lai, Y, Lee, C, Shu, Y, Wang, C: Microwave-assisted rapid fabrication of $Co_3O_4$ nanorods and application to the degradation of phenol. Catal. Today **131**, 105–110 (2008)
30. Bhatt, AS, Bhat, DK, Tai, C-W, Santosh, MS: Microwave-assisted synthesis and magnetic studies of cobalt oxide nanoparticles. Mater. Chem. Phys. **125**, 347–350 (2011)
31. Wang, X, Chen, XY, Gao, LS, Zheng, HG, Zhang, Z, Qian, YT: One-dimensional arrays of $Co_3O_4$ nanoparticles: synthesis, characterization, and optical and electrochemical properties. J. Phys. Chem. B **108**, 16401–16404 (2004)
32. Traversa, E, Sakamoto, M, Sadaoka, Y: A chemical route for the preparation of nanosized rare earth Perovskite-type oxides for electroceramic applications. Part. Sci. Technol. **16**, 185–214 (1998)
33. Salavati-Niasari, M, Davar, F, Mazaheri, M: Preparation of ZnO nanoparticles from [bis(acetylacetonato)zinc(II)]–oleylamine complex by thermal decomposition. Mater. Lett. **62**, 1890–1892 (2008)
34. Salavati-Niasari, M, Davar, F: Synthesis of copper and copper(I) oxide nanoparticles by thermal decomposition of a new precursor. Mater. Lett. **63**, 441–443 (2009)
35. Salavati-Niasari, M, Davar, F, Mazaheri, M: Synthesis and characterization of ZnS nanoclusters via hydrothermal processing from [bis(salicylidene)zinc(II)]. J. Alloys Compd. **470**, 502–506 (2009)
36. Davar, F, Fereshteh, Z, Salavati-Niasari, M: Nanoparticles Ni and NiO: synthesis, characterization and magnetic properties. J. Alloys Compd. **476**, 797–801 (2009)
37. Salavati-Niasari, M, Fereshteh, Z, Davar, F: Synthesis of cobalt nanoparticles from [bis(2-hydroxyacetophenato)cobalt(II)] by thermal decomposition. Polyhedron **28**, 1065–1068 (2009)
38. Salavati-Niasari, M, Khansari, A, Davar, F: Synthesis and characterization of cobalt oxide nanoparticles by thermal treatment process. Inorg. Chim. Acta **362**, 4937–4942 (2009)
39. Salavati-Niasari, M, Mir, N, Davar, F: Synthesis and characterization of $Co_3O_4$ nanorods by thermal decomposition of cobalt oxalate. J. Phys. Chem. Solids **70**, 847–852 (2009)
40. Farhadi, S, Rashidi, N: Preparation and characterization of pure single-phase $BiFeO_3$ nanoparticles through thermal decomposition of the heteronuclear $Bi[Fe(CN)_6]{\cdot}5H_2O$ complex. Polyhedron **29**, 2959–2965 (2010)
41. Farhadi, S, Roostaei-Zaniyani, Z: Simple and low-temperature synthesis of NiO nanoparticles through solid-state thermal decomposition of the hexa(ammine)Ni (II) nitrate, $[Ni(NH_3)_6](NO_3)_2$, complex. Polyhedron **30**, 1244–1249 (2011)
42. Farhadi, S, Safabakhsh, J: Solid-state thermal decomposition of the $[Co(NH_3)_5CO_3]NO_3{\cdot}0.5H_2O$ complex: a simple, rapid and low-temperature synthetic route to Co3O4 nanoparticles. J. Alloys Compd. **515**, 180–185 (2012)
43. Farhadi, S, Pourzare, K: Simple and low-temperature preparation of $Co_3O_4$ sphere-like nanoparticles via solid-state thermolysis of the $[Co(NH_3)_6](NO_3)_3$ complex. Mater. Res. Bull. **47**, 1550–1556 (2012)
44. Nakamoto, K: Infrared and Raman Spectra of Inorganic and Coordination Compounds, Part B: Applications in Coordination, Organometallic, and Bioinorganic Chemistry, 6th edn. Wiley, New York (2009)
45. Pejova, B, Isahi, A, Najdoski, M: Fabrication and characterization of nanocrystalline cobalt oxide thin films. Mater. Res. Bull. **36**, 161–170 (2001)
46. Klug, HP, Alexander, LE: X-ray Diffraction Procedures, 2nd edn. Wiley, New York (1964)
47. Marinkovic Stanojevic, ZV, Romcevic, N, Stojanovic, B: Spectroscopic study of spinel $ZnCr_2O_4$ obtained from mechanically activated $ZnO–Cr_2O_3$ mixtures. J. Eur. Ceram. Soc. **27**, 903 (2007)
48. Ramana, CV, Massot, M, Julien, CM: XPS and Raman spectroscopic characterization of $LiMn_2O_4$ spinels. Surf. Interface Anal. **37**, 412 (2005)
49. Hadjiev, VG, Iliev, MN, Vergilov, IV: The Raman spectra of $Co_3O_4$. J. Phys. C. Solid State Phys. **21**, L199 (1988)
50. Cao, B, Cai, W, Duan, G, Li, Y, Zhao, Q, Yu, D: Template-free electrochemical deposition route to ZnO nanoneedle arrays and their optical and field emission properties. Nanotechnology **16**, 2567 (2005)
51. He, T, Chen, DR, Jiao, XL, Wang, YL, Duan, YZ: Solubility-controlled synthesis of high-quality $Co_3O_4$ nanocrystals. Chem. Mater. **17**, 4023–4030 (2005)
52. Gulino, A, Dapporto, P, Rossi, P, Fragala, I: A novel self-liquid MOCVD precursor for $Co_3O_4$ thin films. Chem. Mater. **15**, 3748–3752 (2003)
53. Ichiyanagi, Y, Kimishima, Y, Yamada, S: Magnetic study on $Co_3O_4$ nanoparticles. J. Magn. Magn. Mater. **272–276**, e1245–e1246 (2004)
54. Kodama, RH, Makhlouf, SA, Berkowitz, AE: Growth mechanism and magnon excitation in NiO nanowalls. Phys. Rev. Lett. **79**, 1393–1396 (1997)
55. Ozkaya, T, Baykal, A, Toprak, MS, Koseoglu, Y, Durmus, Z: Reflux synthesis of $Co_3O_4$ nanoparticles and its magnetic characterization. J. Magn. Magn. Mater. **321**, 2145–2149 (2009)
56. Liszka-skoczylas, M, Mikuli, E, Szklarzewicz, J, Hetmanczyk, J: Thermal behaviour, phase transition and molecular motions in $[Co(NH_3)_6](NO_3)_2$. Thermochim. Acta **496**, 38–44 (2009)

doi:10.1186/2193-8865-3-16
**Cite this article as:** Farhadi *et al.*: **Simple preparation of ferromagnetic $Co_3O_4$ nanoparticles by thermal dissociation of the $[Co^{II}(NH_3)_6](NO_3)_2$ complex at low temperature.** *Journal Of Nanostructure in Chemistry* 2013 **3**:16.